Mon. Not. R. Astron. Soc. **000**, 000–000 (0000) Printed 2 October 2014 (MN LATEX style file v2.2)

The star formation activity in cosmic voids

E. Ricciardelli[1⋆], A. Cava[2], J. Varela[3], V. Quilis[1,4]
[1] *Departament d'Astronomia i Astrofisica, Universitat de Valencia, c/ Dr. Moliner 50, E-46100 - Burjassot, València, Spain*
[2] *Observatoire de Genève, Université de Genève, 51 Ch. des Maillettes, 1290 Versoix, Switzerland*
[3] *Centro de Estudios de Física del Cosmos de Aragón (CEFCA), Plaza San Juan 1, 44001 Teruel, Spain*
[4] *Observatori Astronòmic, Universitat de València, E-46980 Paterna, València, Spain*

arXiv:1410.0023v1 [astro-ph.GA] 30 Sep 2014

Accepted ... Received ...; in original form ...

ABSTRACT

Using a sample of cosmic voids identified in the Sloan Digital Sky Survey Data Release 7, we study the star formation activity of void galaxies. The properties of galaxies living in voids are compared with those of galaxies living in the void shells and with a control sample, representing the general galaxy population. Void galaxies appear to form stars more efficiently than shell galaxies and the control sample. This result can not be interpreted as a consequence of the bias towards low masses in underdense regions, as void galaxy subsamples with the same mass distribution as the control sample also show statistically different specific star formation rates. This highlights the fact that galaxy evolution in voids is slower with respect to the evolution of the general population. Nevertheless, when only the star forming galaxies are considered, we find that the star formation rate is insensitive to the environment, as the main sequence is remarkably constant in the three samples under consideration. This fact implies that environmental effects manifest themselves as fast quenching mechanisms, while leaving the non-quenched galaxies almost unaffected, as their star formation activity is largely regulated by the mass of their halo. We also analyse galaxy properties as a function of void-centric distance and find that the enhancement in the star formation activity with respect to the control sample is observable up to a radial distance $1.5 \cdot R_{void}$. This result can be used as a suitable definition of void shells. Finally, we find that larger voids show an enhanced star formation activity in the shells with respect to their smaller counterparts, that could be related to the different dynamical evolution experienced by voids of different sizes.

Key words: galaxies: evolution – – cosmology: observations– large-scale structure of Universe

1 INTRODUCTION

Large redshift surveys (York et al. 2000; Colless et al. 2001) and cosmological simulations (Bond, Kofman, & Pogosyan 1996; Aragón-Calvo et al. 2010; Cautun et al. 2014) have revealed that galaxies are distributed inside a cosmic web of walls, filaments and compact clusters. Such a web encloses large underdense regions, referred to as cosmic voids.

Voids were first recognized in the earliest redshift surveys (Gregory & Thompson 1978; Kirshner et al. 1981) as huge empty holes in the galaxy distribution. Nowadays, there is a general consensus in that voids occupy most of the volume of the Universe (Sheth & van de Weygaert 2004; van de Weygaert & Platen 2011; Pan et al. 2012) and that they are far from being simple structures. As shown by numerical simulations (van de Weygaert & van Kampen 1993; Sheth & van de Weygaert 2004; Aragon-Calvo & Szalay 2013; Ricciardelli, Quilis, & Planelles 2013), voids host a rich infrastructure, made of subvoids, sheet-like structures and tenuous filaments. These filamentary features have also been observed in the real voids (Beygu et al. 2013; Alpaslan et al. 2014) and are expected to be the favourite sites for galaxy formation in voids (Rieder et al. 2013).

Voids represent a unique and pristine environment for galaxy formation studies, since void galaxies are not affected by the transformation processes (such as ram-pressure stripping, starvation and harassment) that act in groups and clusters. Thus, they allow one to study galaxy evolution as a result of nature only, in the absence of nurture.

In the general environment, it is widely known that the star formation rate (SFR) depends on local density, with galaxies living in dense regions having their star for-

⋆ E-mail: elena.ricciardelli@uv.es

mation rates strongly reduced with respect to field galaxies (Balogh et al. 1997; Poggianti et al. 1999; Elbaz et al. 2007). Evidence has also emerged showing that this SFR-density relation is largely due to an increasing fraction of passive galaxies in dense environment, whereas the star-forming population does not show any significant trend with the environment (Peng et al. 2010; Wijesinghe et al. 2012). This would suggest that any mechanism responsible for the suppression of the SFR would act on a very short timescale. In the rich clusters, however, there are indications that the SFR of star forming galaxies also depends on density (Vulcani et al. 2010).

One way to shed light into the effect of environment on galaxy evolution is to focus on the rarefied void regions, where the nurture processes are not at work and any environmental trend should be driven by 'in-situ' processes. As revealed by observational studies of statistical samples of voids, galaxies in voids are bluer, have higher specific star formation rates and are of later types than galaxies living in regions at average density (Rojas et al. 2004, 2005; Patiri et al. 2006; von Benda-Beckmann & Müller 2008; Hoyle, Vogeley, & Pan 2012; Kreckel et al. 2012). A steady increase in the star formation activity down to the densities typical of voids has been also observed in the surroundings of the Coma supercluster (Cybulski et al. 2014). However, it is still under debate whether this youthful state of void galaxies has an intrinsic nature or it is just a consequence of the mass bias, since the low-mass galaxies dominate the low-density environments. Patiri et al. (2006) find that the colours of void galaxies are not significantly different than those of wall galaxies of the same morphological type. Likewise, Kreckel et al. (2012), studying a sample of 60 void galaxies from the Void Galaxy Survey (VGS, van de Weygaert et al. 2011) conclude that the void galaxy properties do not differ from those of field galaxies of the same luminosity and morphology. On the other hand, other works (Rojas et al. 2004; Hoyle, Vogeley, & Pan 2012) found that the blueness of void galaxies is still recovered when the galaxy population is divided in morphological types. Thus, the peculiarities of void galaxies can not be interpreted as a simple consequence of the morphology-density relation (Dressler 1980). If this effect is real, it would indicate that galaxy evolution in voids is also environmentally driven, although the environmental effects responsible for galaxy transformations should be necessarily different than those acting in high-density regions.

In this work, we aim at studying the star formation properties of void galaxies, with the largest sample ever used for this purpose, and to shed light onto the peculiarities of void galaxies with respect to the galaxies living in the general environment. We do this by using a published catalogue of voids (Varela et al. 2012), drawn from SDSS and including more than 6000 void galaxies. The structure of the paper is as follows. In Section 2 we introduce our catalogue of void and the galaxy samples used in the analysis, in Section 3 we present our results and conclude in Section 4.

Throughout the paper we adopt the following cosmology: $\Omega_m = 0.3$, $\Omega_\Lambda = 0.7$ and all the relevant quantities are rescaled to h=H_0/100km/s/Mpc.

2 THE DATA

2.1 The SDSS void catalogue

The catalogue of cosmic voids used for the present analysis has been described in Varela et al. (2012). Here, we only give a brief description of the void catalogue and refer to the original work for further details.

The galaxy sample used for void identification has been extracted from the New York University Value-Added Galaxy Catalog[1] (NYU-VACG; Blanton et al. 2005), based on the photometric and spectroscopic catalog of SDSS/DR7[2], complete down to $r \sim 17.77$. To guarantee the homogeneity of the sample and avoid the detection of spurious voids, a catalogue complete down to magnitude $M_r - 5logh = -20.17$ in the redshift range: $0.01 \leqslant z \leqslant 0.12$ has been used. Using this galaxy sample, voids are defined as spherical regions devoid of galaxies. As in Varela et al. (2012), we consider only voids whose radius is larger than $10\,h^{-1}\,Mpc$. The catalogue thus includes 699 voids, which, by definition, can host only galaxies fainter than $M_r - 5log(h) = -20.17$.

We also define shell galaxies as those galaxies lying at a distance $\leqslant 30\,h^{-1}\,Mpc$ from the center of a void. For consistency with the void galaxy catalogue, in the shell catalogue, we only include galaxies fainter than $M_r - 5log(h) = -20.17$. Given the relatively large width of the shell, it might occur that the same galaxy belongs to the overlapping shells of different voids. In these cases, and unless otherwise stated, we associate the given galaxy to the closest void, thus avoiding multiple occurrences of the same galaxy in the catalog.

In the upper panel of Fig. 1 we show the stacked two-dimensional distribution of void and shell galaxies, considering all the 699 voids of the sample. The density of galaxies is represented by the Voronoi tessellation of the galaxy distribution and it clearly shows the lack of galaxies within R_{void}. The Voronoi tessellation has been computed by means of the QHULL procedure in IDL, that constructs convex hulls for a 2d distribution of points. The number of galaxies as a function of the void-centric distance rescaled to the void radius, r/R_{void}, is shown in the lower panel of Fig. 1. The sharp increase in the number of galaxies towards the void edge reflects the shape of the void density profile (Ricciardelli, Quilis, & Varela 2014). For the largest voids in the sample, the physical distance of $30\,h^{-1}\,Mpc$, used to define the shell galaxies, corresponds to a rescaled distance $r \sim 1.5 \cdot R_{void}$. Hence, only small voids contain shells larger than this value, resulting in the decaying distribution at $r > 1.5 \cdot R_{void}$ seen in Fig. 1. In the following, shell galaxies out to $30\,h^{-1}\,Mpc$ are considered only when studying trends with the void-centric distance (see 3.3 and 3.4). The rest of the analysis is restricted to galaxies having $r \leqslant 1.5 \cdot R_{void}$.

In addition to the void and shell catalogues, we also build a control sample, including all galaxies fainter than $M_r - 5log(h) = -20.17$ and within the same redshift range of the void sample: $0.01 \leqslant z \leqslant 0.12$. A summary of the samples used in this work is given in Table 1.

We notice that, due to our definition of voids and void galaxies, we can study the environmental effect of voids only

[1] http://sdss.physics.nyu.edu/vagc/
[2] http://cas.sdss.org/astrodr7/en

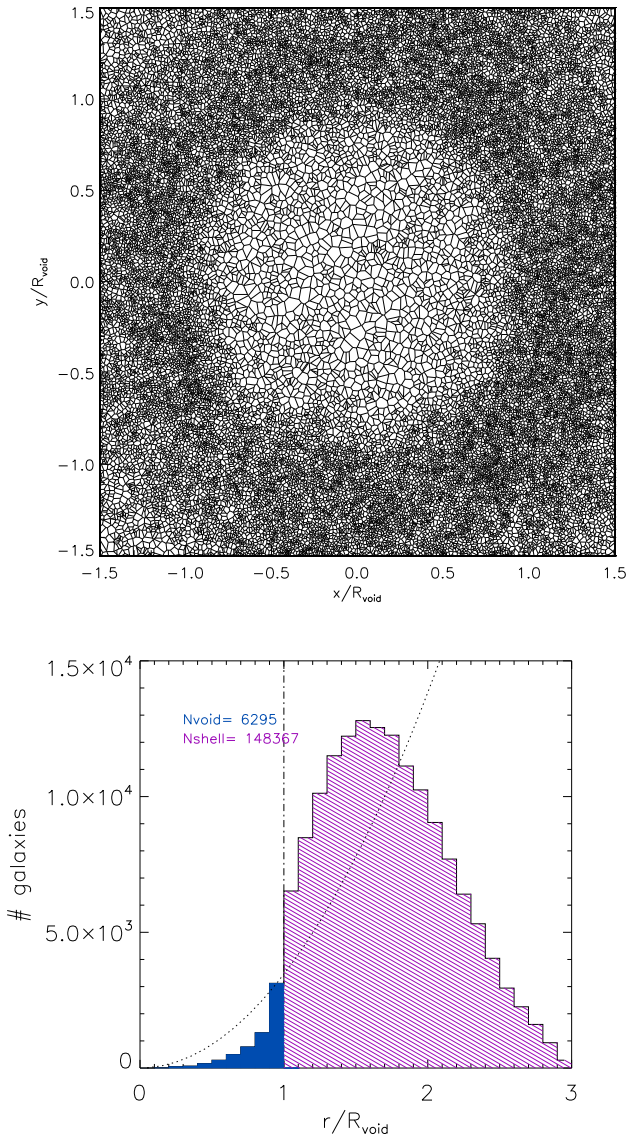

Figure 1. *Upper panel:* two-dimensional representation of the stacked void in comoving coordinates, normalized to the size of the void. A slice of thickness $0.5 \cdot R_{void}$ within the void center has been considered for projection. The cells represent the Voronoi tessellation of the two-dimensional distribution of void and shell galaxies. *Lower panel:* Number of galaxies as a function of their void-centric distance, normalized to the size of the void hosting the galaxies. The sharp increase of the number of galaxies at the void wall ($r/R_{void} \sim 1$, vertical line) is clearly seen. We also show, for comparison, the number of galaxies expected for a sphere of constant density, where the increasing number of galaxies with radius depends only on the increasing volume of the shells. Here and in the following plots, blue refers to void galaxies and magenta indicates the shell galaxies.

on faint galaxies. However, this is not a limitation to our analysis, as dwarf galaxies and low mass galaxies in general, are those showing the greatest peculiarities (Pustilnik et al. 2011, 2013; Cybulski et al. 2014) with respect to galaxies living in higher density environment.

Table 1. Galaxy samples used in this work.

Sample	N_{total} [a]	N_{clean} [b]
Void sample	7210	6295
Shell sample ($r \leqslant 30\,h^{-1}\,Mpc$)	171873	148367
Shell sample ($r/R_{void} \leqslant 1.5$)	56477	48856
Control sample	225822	195222

[a] N_{total} refers to the number of galaxies in the sample fainter than $M_r - 5log(h) = -20.17$ and with redshift in the range $0.01 \leqslant z \leqslant 0.12$.
[b] N_{clean} refers to the number of galaxies in the sample, excluding AGN, LINER and *unclassifiable* objects

2.2 Star formation rates and stellar masses

The SFR and stellar mass estimates used in this paper are those from the MPA catalogue[3] (Brinchmann et al. 2004). The SFR measurements combine a spectroscopic determination of the SFR within the fiber with a photometric one outside it. The SFRs within the fiber are derived from the emission lines, and are primarily based on the intensity of the H_α line. The observed spectra are fitted with a grid of template models, which combine the stellar population models from Bruzual & Charlot (2003) with emission line modelling from Charlot & Longhetti (2001). Dust attenuation is also taken into account by considering the Charlot & Fall (2000) extinction law. The procedure thus produces dust-corrected SFR. Since the SDSS spectra come from a 3" fiber, aperture corrections are needed to account for the missing flux outside the fiber. To estimate it, stellar population models are used to fit the observed photometry and infer the SFR. The total SFR is thus given by summing the SFR in the fiber and the one from the photometry. The stellar masses presented in the MPA catalogue, and used in this work, are those measured in Kauffmann et al. (2003). SFRs and stellar masses are computed assuming a Kroupa (2001) initial mass function.

In addition, the Brinchmann et al. (2004) catalogue provides a spectral classification, based on emission lines (BPT diagrams, Baldwin, Phillips, & Terlevich 1981), useful to separate star-forming galaxies from AGN. To avoid having our SFRs contaminated by the presence of AGN, we exclude from the samples galaxies classified as AGN or LINER according to the Brinchmann classification. We also exclude galaxies classified as *unclassifiable*. In Table 1 we report the number of galaxies in each sample. In all the samples, the number of galaxies excluded because AGN, LINER or *unclassifiable*, contribute by $\sim 13\%$ to the total number of galaxies.

2.3 Correction for incompleteness

The spectroscopic completeness limit of the SDSS DR7 survey (m_r <17.77) implies a redshift-dependent absolute magnitude limit. Hence, our galaxy samples, being fainter than

[3] http://www.mpa-garching.mpg.de/SDSS/DR7/

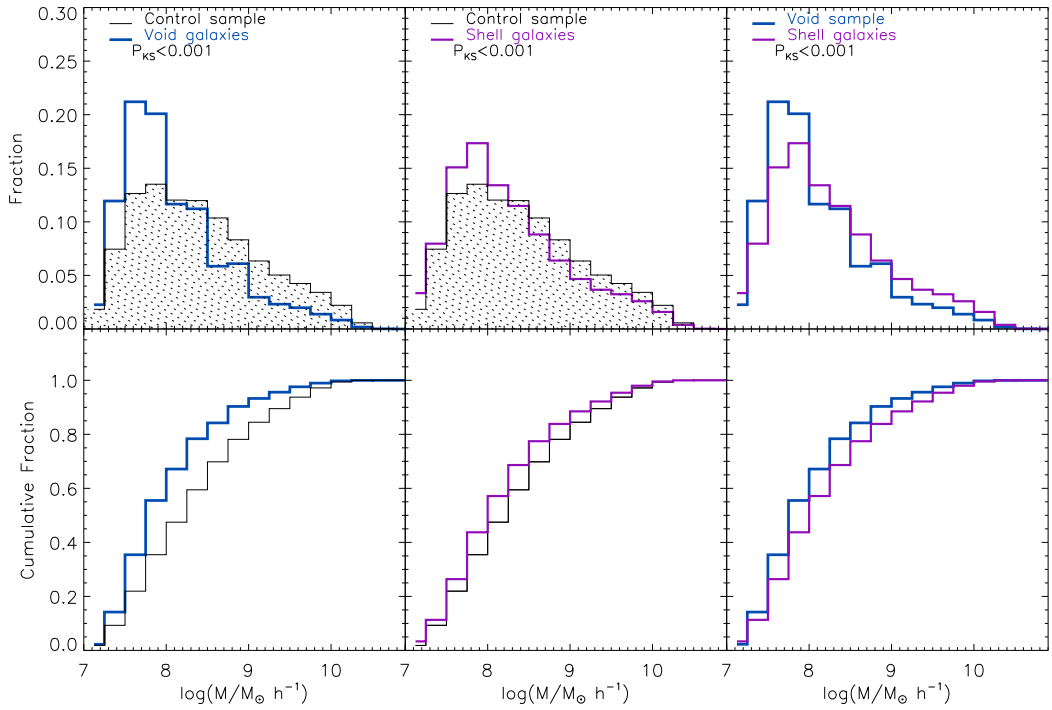

Figure 2. Upper (lower) panels: differential (cumulative) stellar mass distributions for void galaxies (blue), shell galaxies (magenta) and control sample (black). In each panel, the probability that the two distributions are identical according to the Kolmogorov Smirnov test is indicated. The null hypothesis that the two distributions are identical can be rejected in all the cases.

$-20.17 + 5\log(h)$, are not complete and we need to correct for this Malmquist bias. In order to account for this drawback, we correct the sample by weighting each galaxy by $1/V_{max}$ values, where V_{max} is the volume out to the comoving distance at which the galaxy would still be observable.

Broadly speaking, we perform the following steps. The apparent magnitude limit $m_r = 17.77$ of the survey can be translated into a redshift-dependent absolute magnitude (see Appendix of van den Bosch et al. 2008) in the absolute frame at z=0.1:

$$^{0.1}M_r - 5\log(h) = m_r - DM(z) - k_{0.1}(z) + 1.62(z-0.1) - 0.1 \quad (1)$$

where $DM(z)$ is the distance modulus, $k_{0.1}(z)$ is the K-correction to z=0.1, whose redshift dependence can be approximated by (Blanton & Roweis 2007):

$$k_{0.1}(z) = 2.5\log\left(\frac{z+0.9}{1.1}\right) \quad (2)$$

and the term -0.1 at the end of the expression takes into account the scatter in the K-correction. Hence, for each galaxy in the sample, we consider its rest-frame $^{0.1}M_r$ from the NYU-VAGC catalogue and compute the maximum redshift, z_{max} at which the galaxy would be brighter than $m_r = 17.77$. The comoving volume enclosed between z=0.01 and z_{max} gives V_{max}. The weights are finally given by:

$$w_i = \frac{1}{V_{max} C} \quad (3)$$

where C is the spatially-dependent spectroscopic completeness factor, available from the NYU-VAGC. Thus, w_i gives the number of objects per unit volume in a complete sample.

3 RESULTS

3.1 Distributions in galaxy properties

One method to discriminate the environmental effect on galaxy evolution is to compare the distribution of galaxy properties in the different environments. In Figs. 2-4 we show the distribution of stellar mass, SFR and specific star formation rate, $sSFR = SFR/M_*$, of the three samples: voids, shells and control sample. It is worth to notice that the probability density functions (PDF) are calculated using the weights described in Sect. 2.3. Without such weighting scheme, the contribution of low-mass objects would be extremely reduced. Here we focus the analysis of the shell sample only on those galaxies lying at a void-centric distance $\leqslant 1.5 \cdot R_{void}$, in order to highlight any environmental effect with respect to the control sample, that at larger distances is diluted.

Voids have a mass distribution more abundant in low-mass galaxies then shells and control sample (Fig. 2). A two-dimensional Kolmogorov-Smirnov (KS, Peacock 1983) test returns a low probability ($P < 0.001$) that the two distributions are drawn from the same sample. Control sample and shells display mass distribution apparently alike, although the KS test again rejects the null hypothesis that they are drawn from the same distribution. We notice that the same low probabilities are obtained also when using the MannWhitney U test (Mann & Whitney 1974) in all the cases presented in this section.

Concerning the star formation properties, we see that low density regions host galaxies with low star formation

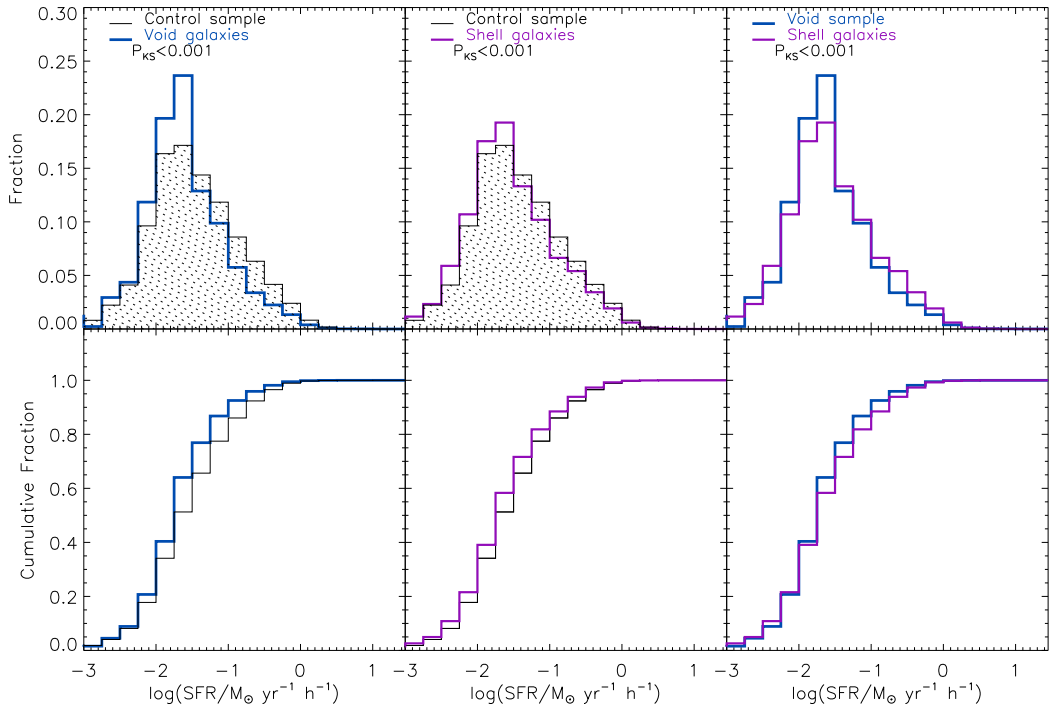

Figure 3. Differential and cumulative SFR distributions for void galaxies (blue histograms), shell galaxies (magenta histograms) and control sample (grey histograms). Colors are coded as in Fig. 2.

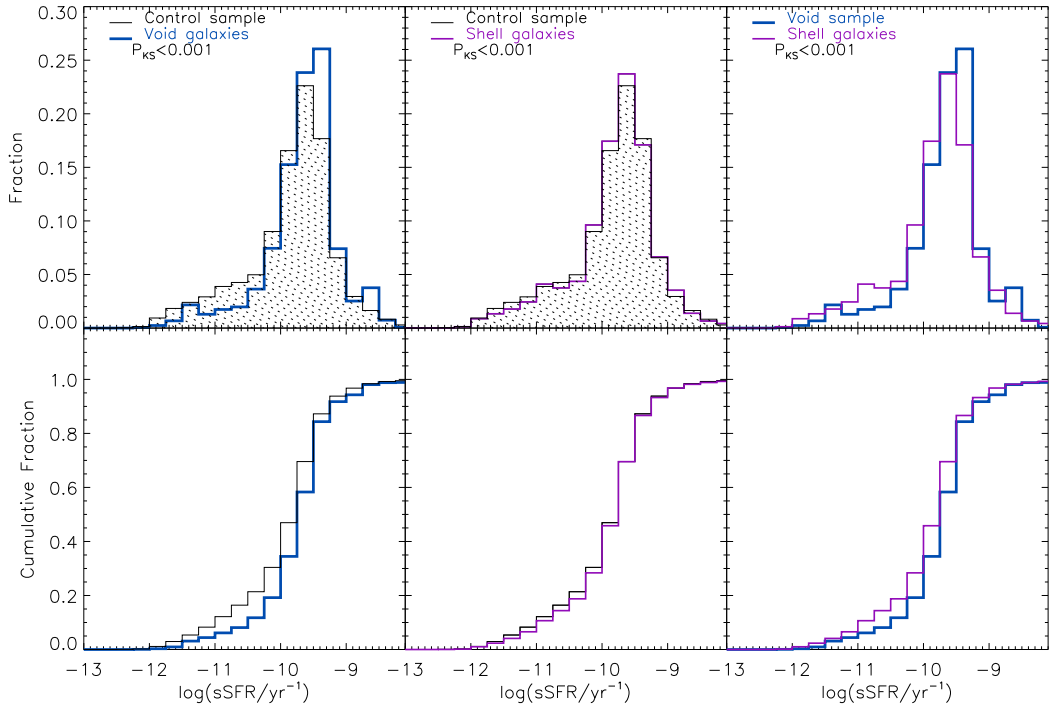

Figure 4. Differential and cumulative sSFR distributions for void galaxies, shell galaxies and control sample. Colors are coded as in Fig. 2.

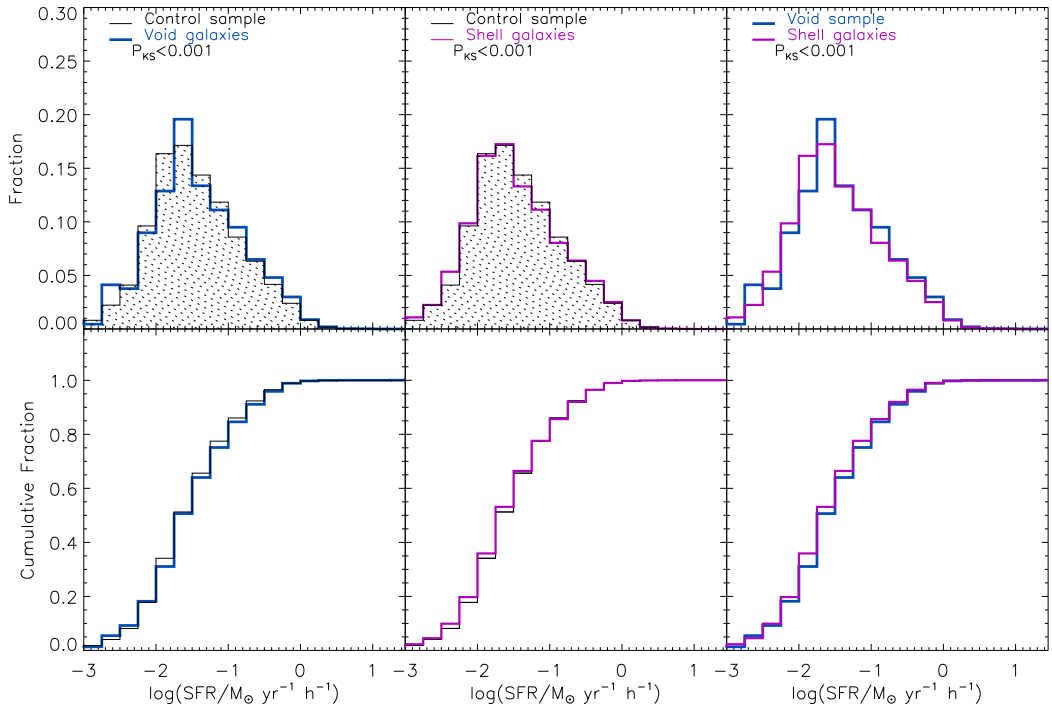

Figure 5. Differential (upper panels) and cumulative (lower panels) SFR distributions of the three samples, using mass-matched samples for the void and shell galaxies, in order to avoid the bias induced by different mass distributions. See text for further details. Colors are coded as in Fig. 2.

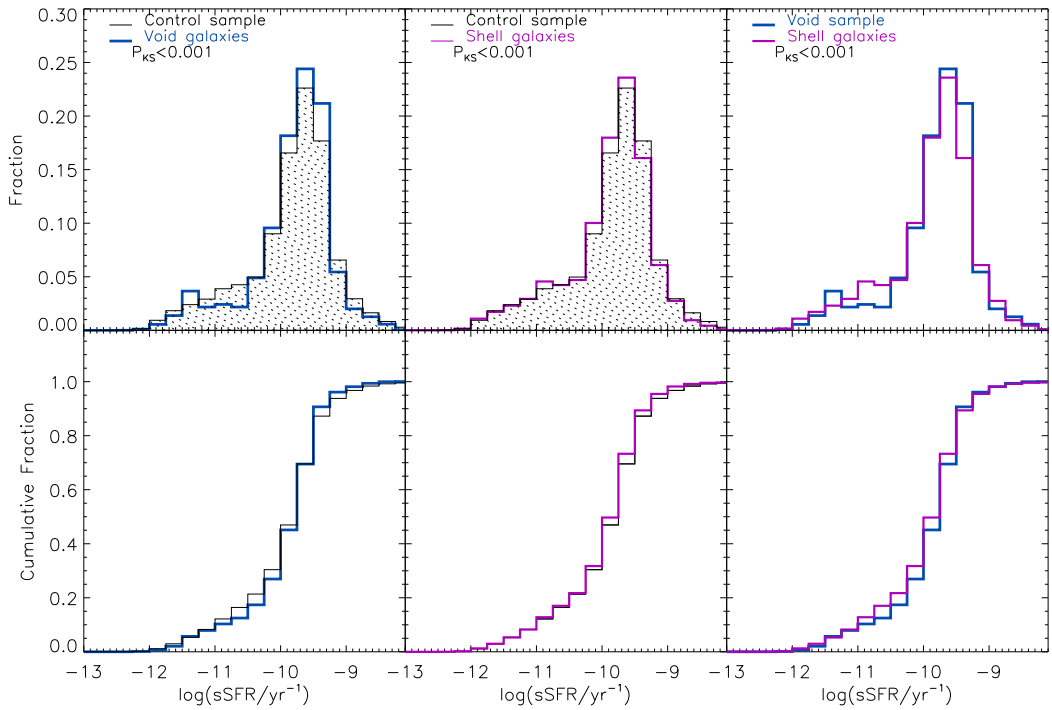

Figure 6. Differential (upper panels) and cumulative (lower panels) sSFR distribution of the three samples, using mass-matched samples for the void and shell galaxies. Colors are as in Fig. 2.

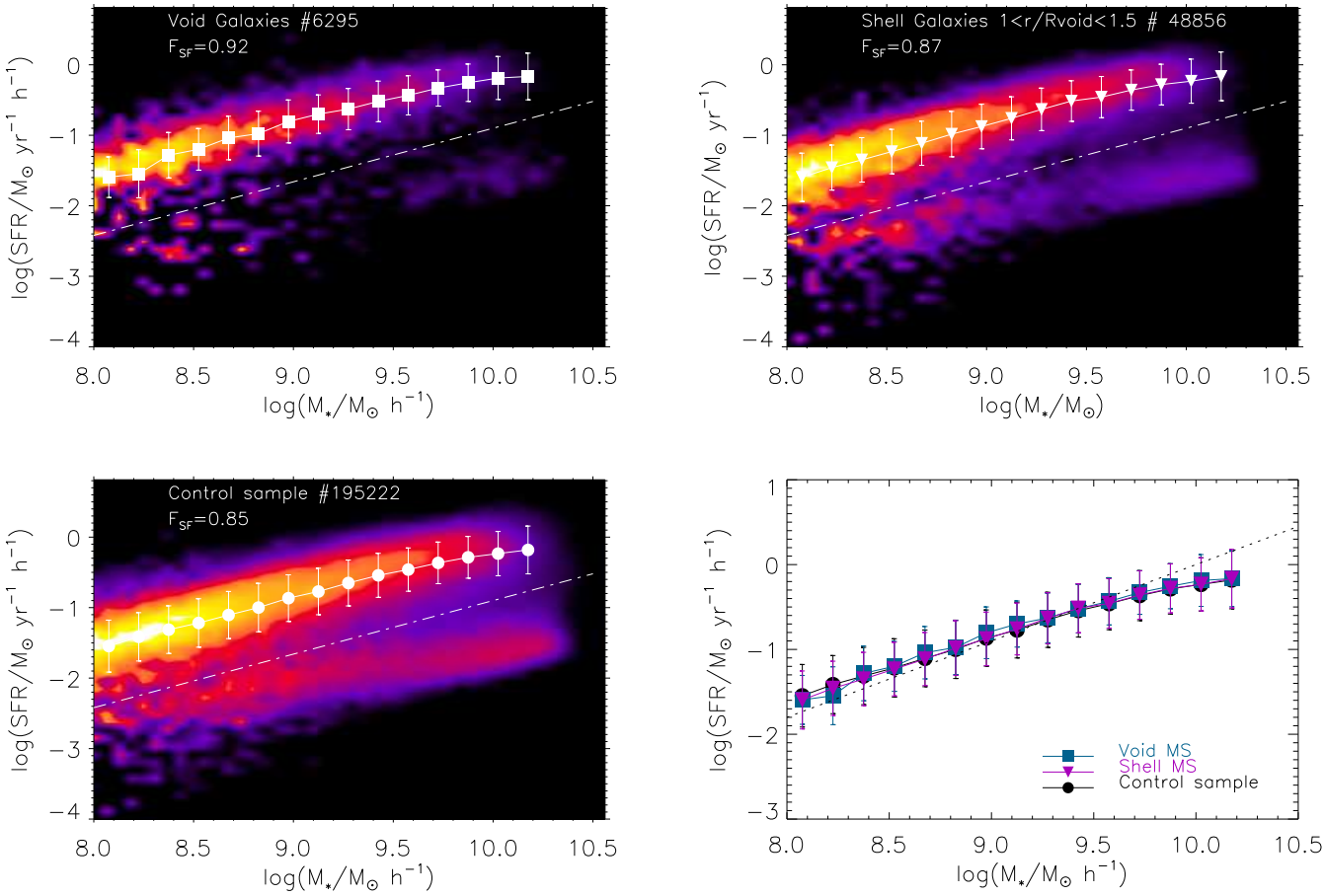

Figure 7. SFR−stellar mass diagram for void galaxies (upper-left panel), shell galaxies with void-centric distance below $1.5 \cdot R_{void}$ (upper-right panel) and the control sample (lower-left panel). Colors indicate the value of the two-dimensional weighted PDF, with yellow-white representing the highly populated regions and purple the poorly populated ones. The dash-dotted line indicates the separation between the star forming and the quiescent regions (Eq. 4). The mean SFR per mass bin for the star forming population is shown by symbols with error-bars, indicating the standard deviation. In the lower-right panel we report the MS of all three environments for comparison. The dotted line is the MS determination from Peng et al. (2010).

rates (Fig. 3), a trend that could be driven by the different mass distributions and the tight correlation existing between SFR and stellar mass (see Sect. 3.2). When focusing on the specific star formation rate (Fig. 4), that gives a measure of the galaxy build-up time, we see that void galaxies form stars more efficiently, as their sSFRs are significantly larger than those of shell and control galaxies. The sSFRs of the shell galaxies are also statistically larger than the control sample. In all the environments, we observe a strong peak at sSFR$\sim 10^{-9.5} yr^{-1}$, representing the star forming galaxies, and a tail at low sSFR representing the passive population, that is not well represented in our sample. Thus, the star forming and passive loci are found at similar sSFR values in all three environments, but the relative fraction of galaxies that populate the two loci varies between the environments.

Although the star formation distributions in voids and shells appear remarkably different than those in the control sample, we can not exclude that this result is just a consequence of the mass bias. Indeed, voids and shells host a larger number of low-mass galaxies with respect to the control sample (see Fig. 2), which may in principle bias the SFR and sSFR distributions. To avoid the influence of the mass distribution, we have randomly extracted 10 subsamples from the void and the shell samples, having the same mass distribution of the control sample. In Figs. 5-6 we show the SFR and sSFR distributions for these mass-matched samples of voids and shells, compared with the original control sample. We do not show the mass distributions, as they are, by construction, identical to each other. The SFR distributions in this case appear remarkably similar, indicating that the low values of SFR in voids are mainly due to the predominance of low mass galaxies. However, the sSFR trend with environment is still recovered, showing that the void galaxies have the passive population strongly suppressed with respect to the control sample, whereas shell and control galaxies have similar sSFR distributions.

3.2 Main Sequence

A tight correlation between the star formation rate and the stellar mass has been observed both in the local Universe (Brinchmann et al. 2004; Salim et al. 2007; Peng et al.

2010) and at high redshift (Noeske et al. 2007; Elbaz et al. 2007; Rodighiero et al. 2010, 2014), widely known as the Main Sequence (MS).

In Fig. 7 we show how the galaxies of our samples are distributed in the SFR - stellar mass plane. The colors indicate the value of the two-dimensional weighted probability distribution function (PDF). All the environments show two separate sequences: a well-defined main sequence at high SFR and a cloud at low star formation formed by the quiescent galaxies. These two sequences are analogous to the blue cloud and the red sequence observed in the colour-magnitude diagram (Strateva et al. 2001; Baldry et al. 2004). This bimodality motivates the division into star forming and quiescent galaxies. In order to separate the two populations, we compute the SFR distributions in small mass intervals. From the bimodal SFR distributions at each mass bin, it is possible to define a minimum SFR, located in the valley between the low- and high-SFR peaks. These minima give the separating line between star forming and passive galaxies:

$$\log(SFR) = 0.76\log(M) - 8.5 \quad (4)$$

and it is shown by the dash-dotted line in Fig. 7. We have applied this procedure to the control sample and used the same definition of star forming galaxies for all the three samples. We notice that, when translated into sSFR, our definition is in perfect agreement with the one adopted by Omand, Balogh, & Poggianti (2014). All the galaxies lying above this line can be defined as star forming and used to define the MS, given by the mean SFR in each stellar mass interval. In the bottom-right panel of Fig. 7 we show the comparison between the MS in the three different environments, and we find that they are completely consistent with each other and with the relation of Peng et al. (2010), which was measured for the general environment with SDSS data. A similar scatter ($\sim 0.3dex$) is also found for the three samples.

Although in rich clusters, the MS has been claimed to depend on the local density (Vulcani et al. 2010), in the field it has been shown to be independent of the environment (Peng et al. 2010). Our results thus show that this is also valid down to the extreme low densities of cosmic voids (see also Kreckel et al. 2012).

3.3 Galaxy properties vs void-centric distance

In this section we investigate how galaxy properties depend on the galaxy position within the void. In Fig. 8 we show how the fraction of star forming galaxies depends on the void-centric distance, normalized to the void size. Star forming galaxies are defined as those galaxies lying above the line defined in Eq. 4. The confidence interval has been estimated by means of 1000 bootstrap resamplings. We find that the fraction of star forming galaxies in the innermost part of the void is close to 1 and then it steadily decreases as moving to large distances from the void center. Interestingly, the star forming fraction converges to the mean value measured for the control sample for distance $r \geqslant 1.5{\cdot}R_{void}$. When splitting the sample in low- and high-mass galaxies, we still observe a significant decrease in the star forming fraction in the two sub-samples, indicating that the trend is not simply driven by an increase of the mean galaxy mass towards the void edge. In the low-mass sample, the decaying appears milder,

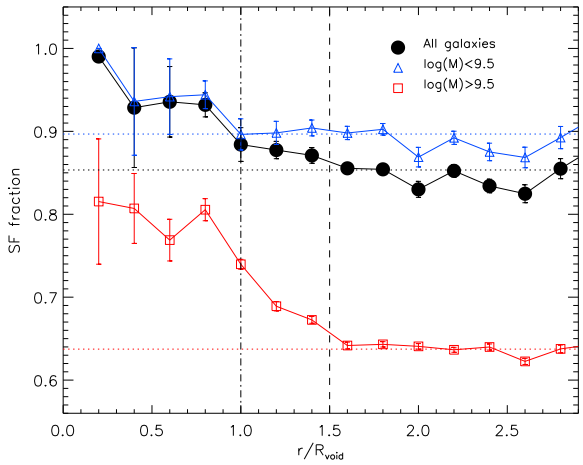

Figure 8. Fraction of star forming galaxies as a function of void-centric distance for all (black circles), low-mass ($\log(M) \leqslant 9.5$, blue triangles) and high-mass galaxies ($\log(M > 9.5$ red squares). Error-bars denote the 1σ confidence intervals computed by means of 1000 bootstrap resamplings. The horizontal lines indicate the star forming fraction in the general sample. The vertical lines indicate the position of the void edge (dot-dashed line) and the value: $r/R_{void} = 1.5$ where the shell properties converge to those of the control sample (dashed line).

as the vast majority of low-mass galaxies are star forming in all the environments. The convergence to the star forming fraction of the control value for $r \geqslant 1.5 \cdot R_{void}$ holds also for the two sub-samples.

In Fig. 9 we show how galaxy properties, namely M_*, SFR and sSFR, change with the void-centric distance. We find lower stellar masses and lower SFRs in the central region of the void, although the errorbars are too large to draw robust conclusion. On the other hand, the sSFR of the main sample appears to decrease at large distances, pointing towards a progressive reduction of the star formation activity of the global sample. Although the trend of the sSFR with respect to the void-centric distance appears in contradiction with the behavior of the SFR that increases at large distances, the latter quantity is well correlated with the stellar mass (see Sect. 3.2) which is driving the SFR trend with void-centric distance.

The progressive reduction in the star formation activity with the void-centric distance can be interpreted as a manifestation of the SFR-density relation within void regions, ought to an increasing local density approaching the void edge, as shown by the void density profiles (Colberg et al. 2005; Ricciardelli, Quilis, & Planelles 2013; Ricciardelli, Quilis, & Varela 2014). The convergence of galaxy properties to the control sample value allows us to define the region of influence of voids as extending up to $1.5 \cdot R_{voids}$.

3.4 Galaxy properties vs void size

In this section, we explore whether the star formation activity in voids and void shells depends on the size of the voids. The void sample has been divided into four equally-populated subsamples at different radii, containing $\sim$ 175

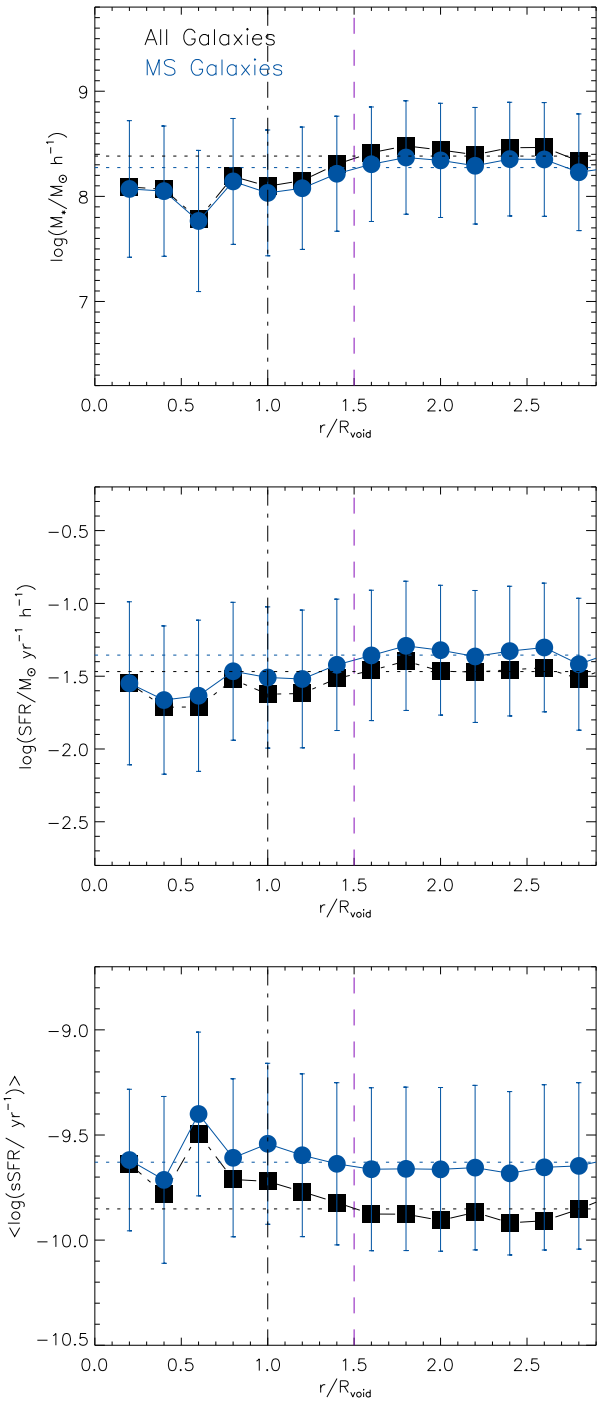

Figure 9. Galaxy properties as a function of void-centric distance. From top to bottom we show: stellar mass, SFR and sSFR. Black squares indicate the mean values for the whole sample, whereas blue circles stay for the main sequence galaxies. For clearness we only show the standard deviations for the MS samples. Horizontal dotted lines denote the mean quantities in the control sample for all the galaxies (black) and the MS galaxies (blue). Vertical lines indicate the positions of the void edge (black dot-dashed) and the shell limit (purple dashed).

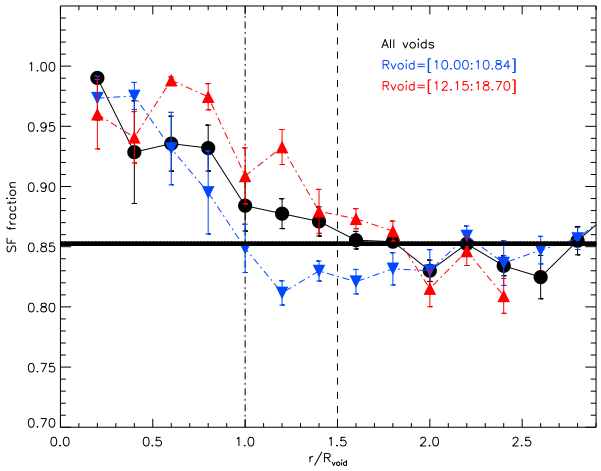

Figure 10. Fraction of star forming galaxies as a function of void-centric distance for voids of different size. The black symbols indicate the whole sample of voids, the blue ones refer to voids in the lowest quartile of the size distribution and the red ones to those in the upper quartile.

voids each. The star formation fraction as a function of the void-centric distance for the two extreme quartiles at small and large void radii is shown in Fig. 10 and compared with the curve of the whole void sample. In the inner part of the voids, the small and large voids do not show significant differences. However, when approaching the void edge ($0.8 \lesssim r/R_{void} \lesssim 1.5$), the two curves start to deviate, with the large voids showing an enhanced star formation activity in their shells with respect to their smaller counterparts. Although the low number statistics prevent us to draw robust conclusions, this result would support the theoretical expectations that small and large voids have different dynamical evolution, that is determined by the large scale region surrounding them (Sheth & van de Weygaert 2004). In support of this, there are evidences that small voids are surrounded by an overdense shell, that in the larger voids is not observed (Ceccarelli et al. 2013, Hamaus, Sutter, & Wandelt 2014, but see also Nadathur et al. 2014).

4 CONCLUSIONS

In this work we have performed a statistical study of the star formation activity in voids and void shells and compared it with a control galaxy sample. As previously observed, we find that void galaxies are characterized by lower stellar masses and enhanced star formation activity with respect to galaxies in the general environment. Shells appear as a transition region, having galaxies with intermediate properties between void galaxies and the general galaxy population. We can exclude that the difference in the sSFR of the three environments under consideration is due to the different mass distributions, as a similar result on the sSFR distribution is obtained when comparing mass-matched sub-samples.

The effect of void environment manifests itself in the different proportion of star forming and passive galaxies, but the average sSFR of the two populations taken separately does not depend on the large-scale environment. This result

is more clearly observed in the star forming main sequence, that is remarkably constant over the three environments. That is to say, when the stellar mass and the population type (star forming or passive) are fixed, the star formation activity does not depend on the environment. This result is consistent with the findings in the general field indicating that there is no strong effect due to local density on the star forming MS (Peng et al. 2010; Wijesinghe et al. 2012). This uniformity of the MS over the large-scale environment would indicate that environmental effects are fast-acting, thus manifesting themselves as quenching mechanisms, that rapidly move the galaxy from the MS to the passive region. Conversely, the regulation of the supply of gas available for star formation in those galaxies that are not quenched, depends largely on the mass of the host halo and has no further relation with environment.

We also find a significant radial variation of the star forming fraction, with the innermost part of voids having the passive population strongly suppressed. Interestingly, the properties related to the void-centric distance converge to the general field values for a fixed radius of $\sim 1.5r/R_{void}$, that can serve as suitable definition of void shell. Furthermore, we observe a different star formation activity in the shells of voids of different sizes, with the small voids having a more abundant passive population with respect to the larger voids. This could be related to the different dynamical evolution experienced by voids of different sizes (Sheth & van de Weygaert 2004; Ceccarelli et al. 2013).

One aspect that still needs to be understood is whether the enhancement in the star formation activity within voids is just a consequence of the SFR-density relation, being the inner regions of voids extremely rarefied (see Ricciardelli et al. 2014), or there is an additional influence of voids beside that of the local density (see Ceccarelli et al. 2008). We plan to test this issue in a future work.

ACKNOWLEDGEMENTS

This work was supported by the Spanish Ministerio de Economía y Competitividad (MINECO, grants AYA2010-21322-C03-01) and the Generalitat Valenciana (grant PROMETEO-2009-103). The work of AC is supported by the STARFORM Sinergia Project funded by the Swiss National Science Foundation. J.V. did part of the work thanks to a post-doc fellowship from the former Spanish Ministry of Science and Innovation under programs 3I2005 and 3I2406. J.V. also acknowledges the financial support from the FITE (Fondos de In versión de Teruel) and the Spanish grant AYA2012-30789. ER acknowledges the kind hospitality of the Observatoire de Genève (Université de Genève) during the preparation of part of this work.

This work has used data from SDSS Data Release 7. Funding for the SDSS and SDSS-II has been provided by the Alfred P. Sloan Foundation, the Participating Institutions, the National Science Foundation, the U.S. Department of Energy, the National Aeronautics and Space Administration, the Japanese Monbukagakusho, the Max Planck Society, and the Higher Education Funding Council for England. The SDSS Web Site is http://www.sdss.org/.

REFERENCES

Alpaslan M., et al., 2014, MNRAS, 440, L106
Aragón-Calvo M. A., Platen E., van de Weygaert R., Szalay A. S., 2010, ApJ, 723, 364
Aragon-Calvo M. A., Szalay A. S., 2013, MNRAS, 428, 3409
Baldry I. K., Glazebrook K., Brinkmann J., Ivezić Ž., Lupton R. H., Nichol R. C., Szalay A. S., 2004, ApJ, 600, 681
Baldwin J. A., Phillips M. M., Terlevich R., 1981, PASP, 93, 5
Balogh M. L., Morris S. L., Yee H. K. C., Carlberg R. G., Ellingson E., 1997, ApJ, 488, L75
Beygu B., Kreckel K., van de Weygaert R., van der Hulst J. M., van Gorkom J. H., 2013, AJ, 145, 120
Blanton M. R., et al., 2005, AJ, 129, 2562
Blanton M. R., Roweis S., 2007, AJ, 133, 734
Bond J. R., Kofman L., Pogosyan D., 1996, Nature, 380, 603
Brinchmann J., Charlot S., White S. D. M., Tremonti C., Kauffmann G., Heckman T., Brinkmann J., 2004, MNRAS, 351, 1151
Bruzual G., Charlot S., 2003, MNRAS, 344, 1000
Charlot S., Fall S. M., 2000, ApJ, 539, 718
Cautun M., van de Weygaert R., Jones B. J. T., Frenk C. S., 2014, MNRAS, 441, 2923
Ceccarelli L., Paz D., Lares M., Padilla N., Lambas D. G., 2013, MNRAS, 434, 1435
Ceccarelli L., Padilla N., Lambas D. G., 2008, MNRAS, 390, L9
Charlot S., Fall S. M., 2000, ApJ, 539, 718
Charlot S., Longhetti M., 2001, MNRAS, 323, 887
Colberg J. M., Sheth R. K., Diaferio A., Gao L., Yoshida N., 2005, MNRAS, 360, 216
Colless M., et al., 2001, MNRAS, 328, 1039
Cybulski R., Yun M. S., Fazio G. G., Gutermuth R. A., 2014, MNRAS, 439, 3564
Dressler A., 1980, ApJ, 236, 351
Elbaz D., et al., 2007, A&A, 468, 33
Gregory S. A., Thompson L. A., 1978, ApJ, 222, 784
Hamaus N., Sutter P. M., Wandelt B. D., 2014, PhRvL, 112, 251302
Hoyle F., Vogeley M. S., Pan D., 2012, MNRAS, 426, 3041
Kauffmann G., et al., 2003, MNRAS, 341, 33
Kirshner R. P., Oemler A., Jr., Schechter P. L., Shectman S. A., 1981, ApJ, 248, L57
Kroupa P., 2001, MNRAS, 322, 231
Kreckel K., Platen E., Aragón-Calvo M. A., van Gorkom J. H., van de Weygaert R., van der Hulst J. M., Beygu B., 2012, AJ, 144, 16
Mann H. B., Whitney D. R., 1947, Ann. Math. Statistics, 18, 50
Nadathur S., Hotchkiss S., 2013, arXiv, arXiv:1310.2791
Nadathur S., Hotchkiss S., Diego J. M., Iliev I. T., Gottlöber S., Watson W. A., Yepes G., 2014, arXiv, arXiv:1407.1295
Noeske K. G., et al., 2007, ApJ, 660, L47
Omand C. M. B., Balogh M. L., Poggianti B. M., 2014, MNRAS, 440, 843
Pan D. C., Vogeley M. S., Hoyle F., Choi Y.-Y., Park C., 2012, MNRAS, 421, 926

Peng Y.-j., et al., 2010, ApJ, 721, 193
Patiri S. G., Prada F., Holtzman J., Klypin A., Betancort-Rijo J., 2006, MNRAS, 372, 1710
Peacock J. A., 1983, MNRAS, 202, 615
Poggianti B. M., Smail I., Dressler A., Couch W. J., Barger A. J., Butcher H., Ellis R. S., Oemler A., Jr., 1999, ApJ, 518, 576
Pustilnik S. A., Martin J.-M., Lyamina Y. A., Kniazev A. Y., 2013, MNRAS, 432, 2224
Pustilnik S. A., Martin J.-M., Tepliakova A. L., Kniazev A. Y., 2011, MNRAS, 417, 1335
Ricciardelli E., Quilis V., Planelles S., 2013, MNRAS, 434, 1192
Ricciardelli E., Quilis V., Varela J., 2014, MNRAS, 440, 601
Rieder S., van de Weygaert R., Cautun M., Beygu B., Portegies Zwart S., 2013, MNRAS, 435, 222
Rodighiero G., et al., 2014, arXiv, arXiv:1406.1189
Rodighiero G., et al., 2010, A&A, 518, L25
Rojas R. R., Vogeley M. S., Hoyle F., Brinkmann J., 2005, ApJ, 624, 571
Rojas R. R., Vogeley M. S., Hoyle F., Brinkmann J., 2004, ApJ, 617, 50
Salim S., et al., 2007, ApJS, 173, 267
Sheth R. K., van de Weygaert R., 2004, MNRAS, 350, 517
Strateva I., et al., 2001, AJ, 122, 1861
York D. G., et al., 2000, AJ, 120, 1579
van den Bosch F. C., Aquino D., Yang X., Mo H. J., Pasquali A., McIntosh D. H., Weinmann S. M., Kang X., 2008, MNRAS, 387, 79
van de Weygaert R., Platen E., 2011, IJMPS, 1, 41
van de Weygaert R., van Kampen E., 1993, MNRAS, 263, 481
Varela J., Betancort-Rijo J., Trujillo I., Ricciardelli E., 2012, ApJ, 744, 82
von Benda-Beckmann A. M., Müller V., 2008, MNRAS, 384, 1189
Vulcani B., Poggianti B. M., Finn R. A., Rudnick G., Desai V., Bamford S., 2010, ApJ, 710, L1
Wijesinghe D. B., et al., 2012, MNRAS, 423, 3679